



Short Communication

Ligand free copper-catalyzed heterogeneous O-arylation reaction under green condition



Tanmoy Maity, Debraj Saha, Soma Das, Susmita Bhunia, Subratanath Koner*

Department of Chemistry, Jadavpur University, Kolkata 700 032, India

ARTICLE INFO

Article history:

Received 16 June 2014

Received in revised form 30 August 2014

Accepted 1 September 2014

Available online 16 September 2014

Keywords:

Post-synthetic modification

IRMOF-3

Cu(II)

Heterogeneous catalysis

O-arylation

Shape selectivity

ABSTRACT

A highly porous Zn-based iso-reticular metal–organic framework (IRMOF-3) has been selected for covalent modification. Pyridine-2-aldehyde has been used to decorate the free amine group of IRMOF-3 in the porous matrix. Schiff base moiety thus generated has been availed to anchor copper(II) ions to prepare the desired catalyst that catalyzes O-arylation reactions heterogeneously under mild reaction conditions. Porous catalyst demonstrates size selectivity in products when various substrates undergo O-arylation with α and β -naphthol.

© 2014 Elsevier B.V. All rights reserved.

1. Introduction

Diaryl ethers are very important structural motifs in a large number of natural biologically active compounds, for example, K13, perrottetin and vancomycin, as well as in polymer industries [1]. During the last few decades, synthetic chemists have developed numerous systems for constructing diaryl ethers [2]. Both Hartwig et al. and Buchwald et al. have developed Pd-catalyzed C–O cross-coupling reactions to aryl halides and phenols in the mid 1990s and then much progress has been made using Pd/ligand systems [3,4]. While Pd-mediated systems show high efficacy in terms of turnover in cross-coupling reactions, costly and toxic Pd limits its applications to large scale production [3,5]. In the meantime, a cheap catalytic method of Cu-mediated Ullmann coupling has been successfully developed, but the harsh reaction conditions (very high temperature, strong base, long reaction time) and employment of stoichiometric amount of copper restricted its limit [6,7]. Since then, efforts have been devoted to provide the most efficient copper-catalyzed O-arylation methods. To our knowledge, there are only few reports that described copper-based reusable heterogeneous catalytic systems [1,2,8–13].

In the last few decades metal–organic frameworks (MOFs) have attracted extensive interest due to their exceptional features like high porosity, high thermal stability and easy incorporation or modification for employing them in heterogeneous catalytic reactions [14–20]. Application of MOFs in heterogeneous catalysis is promising to find its

niche in research [21,22]. Standing out from the vast majority of metal–organic coordination polymers, iso-reticular metal–organic framework (IRMOF) is the class of highly porous zinc carboxylates discovered by Yaghi et al. [23,24]. Its prototype is IRMOF-1, in which $\{Zn_4O\}$ building blocks are linked together by terephthalate bridges [25]. IRMOF-3 is a known MOF with a cubic topology prepared from $Zn(NO_3)_2 \cdot 4H_2O$ and 2-amino-1,4-benzene dicarboxylic acid (R_3 -BDC) [23]. The only difference in IRMOF-3 is the amine moieties are uncoordinated and lined with the pores of the framework. With the advantage of free amino groups present in the framework anchoring of metal sites in MOF has been facilitated. Thus IRMOF-3 represents a good model system for a post-synthetic covalent modification study [26].

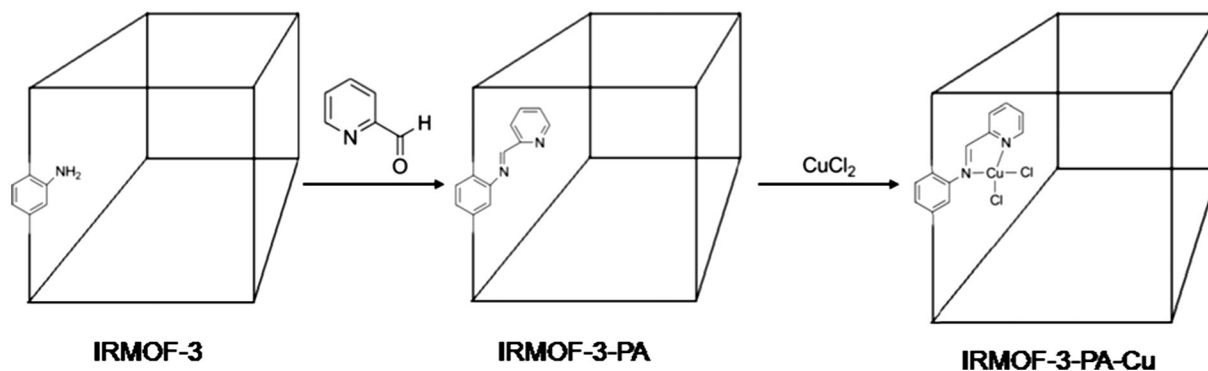
Here we report a facile route for C–O cross-coupling reactions efficiently catalyzed by a heterogeneous system derived from post-synthetic modification of the metal–organic framework, IRMOF-3, and subsequent anchoring of copper(II) into MOF through complex formation (Scheme 1). Notably, the MOF-based catalyst exhibits shape selectivity in product formation by virtue of the restriction of pore size in the framework.

2. Experimental

2.1. Synthesis of IRMOF-3, $[Zn_4O(ATA)_3]$ (ATA = 2-aminoterephthalate) (1)

Bulk sample of IRMOF-3 was prepared by following the procedure described previously [27] and activated by guest exchange with anhydrous $CHCl_3$ solvent. After activation the structure and purity

* Corresponding Author: Tel.: +91 33 2414 6666 Ext. 2778; fax: +91 33 2414 6414.
E-mail address: snkoner@chemistry.jdvu.ac.in (S. Koner).



Scheme 1. Schematic diagram for preparation of 3.

of the material was checked by powder XRD and compared with the pattern reported in literature [27]. Yield 63% (average). Elemental analysis of $Zn_4O(ATA)_{2.61}$: calcd, C 35.37%, H 1.86%, N 5.16%; found, C 35.41%, H 1.90%, N 5.19%. IR (KBr, cm^{-1}): 3438, 1565, 1418, 1392, 1249, 1022, 753 (Fig. 1).

2.2. Synthesis of IRMOF-3-PA, $[Zn_4O(ATA)_3 - x(PITE)_x]$ (PITE = 2-pyridyl-imine terephthalate) (2)

IRMOF-3 was modified by pyridine-2-aldehyde (5 mmol, 0.535 g) in 15 mL of dry CH_3CN as described previously [26]. Elemental analysis of $Zn_4O(ATA)_{2.61}(PITE)_{0.39}$: calcd, C 37.23%, H 1.92%, N 5.59%; found, C 37.19%, H 1.90%, N 5.57% (13% amine functionalization). IR (KBr, cm^{-1}): 3442, 1651, 1617, 1412, 1386, 1254, 1081, 754 (Fig. 1).

2.3. Synthesis of IRMOF-3-PA-Cu, $[Zn_4O(ATA)_3 - x(PITE-CuCl_2)_x]$ (3)

IRMOF-3-PA-Cu was prepared by stirring of 1 g IRMOF-3-PA with 1 mmol (0.17 g) of $CuCl_2 \cdot 2H_2O$ in 15 mL of dry CH_3CN for 8 h under nitrogen atmosphere. The green solid thus formed was filtered and washed by Soxhlet extraction method to remove unanchored copper

species and dried under vacuum at 120 °C. Anal. Calcd. for $Zn_4O(ATA)_{2.61}(PITE-CuCl_2)_{0.39}$ (corresponding to 13% amine functionalization and quantitative copper uptake): calcd., C 35.07%, H 1.81%, N 5.26%; found, C 35.11%, H 1.85%, N 5.29%. The amount of copper in the final solid was determined by the atomic absorption spectrometer: calcd: Cu 2.75 wt.%; found, Cu 2.72 wt.% (4.28×10^{-2} mol%). IR (KBr, cm^{-1}): 3428, 1574, 1390, 751, 485, 417 (Fig. 1). FTIR (cm^{-1}): 364, 306.

2.4. Preparation of PBA-MCM-41

The anchoring of (3-aminopropyl)-triethoxysilane (3-APTES) into MCM-41 had been achieved according to reported method [26]. The prepared yellowish solid PBA-MCM-41 was collected by filtration and dried in desiccator (see Scheme S1 in Supplementary content).

2.5. Preparation of SBA-15-TM-Cu

SBA-15 material was synthesized as reported earlier [28]. 100 mg of calcined SBA-15 was stirred with 0.1 mL of APTES in 20 mL dry chloroform under N_2 atmosphere for 12 h. The white solid product, NH_2 -SBA-15 was obtained and washed with chloroform. Then NH_2 -SBA-15 was refluxed with 0.1 mL of salicylaldehyde (SA) in methanol for 8 h and a yellow solid product, (SBA-15-TM) was obtained. Finally SBA-15-TM was refluxed with 0.5 mmol of copper chloride in methanol for 16 h and an aqua-green solid (SBA-15-TM-Cu) was obtained (Scheme S2). Excess metal was removed by Soxhlet extraction. PXRD patterns (Figure S1), FTIR (Figure S2), N_2 sorption isotherm (Figure S3) and pore size distribution (Figure S4) clearly justify the modification of mesoporous SBA-15 [29].

2.6. General experimental procedure for the O-arylation coupling reactions

At first aryl halide (1.2 mmol) and Cs_2CO_3 (1 mmol, 0.33 g) were added to solid IRMOF-3-PA-Cu (0.002 g) catalyst in a two neck round bottom flask. To this solid mixture aryl alcohols (1.0 mmol) and 2 mL dry ethanol solvent were added (solid aryl alcohol was added directly with the catalyst) and the reaction mixture was stirred and refluxed at 80 °C in an oil bath under nitrogen atmosphere. After cooling to room temperature, the catalyst was first separated out by centrifugation and the solution part was concentrated directly by rotary evaporator. The residue was purified by column chromatography on silica gel (mesh 60–120) using n-hexane/ethyl acetate mixture as the eluent.

3. Results and discussion

3.1. Characterization

IRMOF-3 is known to be hydrophilic and moisture sensitive [30]. Structural disintegration of IRMOF-3-PA due to presence of crystalline

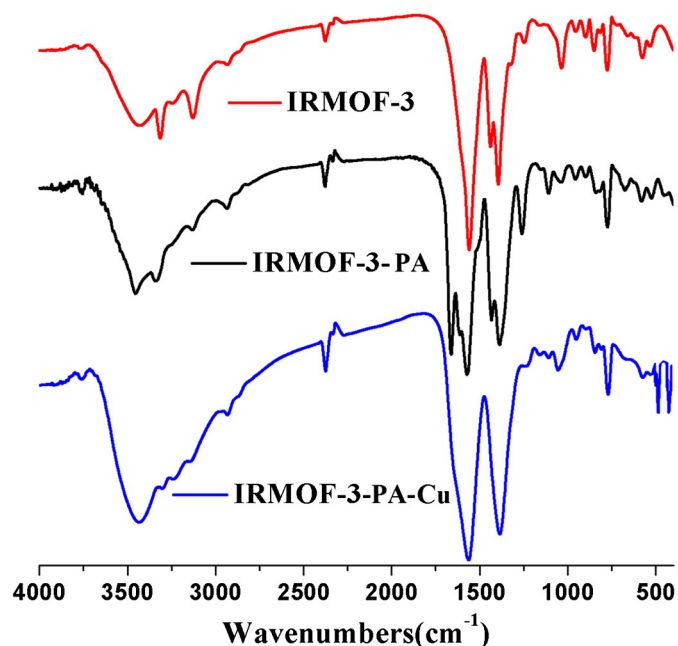


Fig. 1. FTIR spectra of 1, 2 and 3.

water in Cu(II) salt may occur. However, organic modification changes the nature of IRMOF-3 from hydrophilic to hydrophobic [30]. Owing to this the framework system retains its structural integrity after metal incorporation using $\text{CuCl}_2 \cdot 2\text{H}_2\text{O}$. To optimize the extent of modification, we investigate the functionalization of IRMOF-3, by varying the amount of pyridine-2-aldehyde and, subsequently, by varying the amount of copper chloride during Schiff base complex formation stage (Figures S5 and S6).

Solid state UV-vis spectra of both IRMOF-3 and IRMOF-3-PA (Figure S7) featured two strong absorption bands (around 251, 280 and 258, 335 nm respectively), whereas the later one showed an additional transition ~ 382 nm which was attributed to the $\pi-\pi^*$ transition of $\text{C}=\text{N}$ group. IRMOF-3-PA-Cu, however, exhibited an additional weak yet distinct band at ~ 743 nm (Figure S7), which could be ascribed to $d-d$ transition of metal typical for a Cu-Schiff base complex [31].

The FTIR spectra of all three samples were measured (Fig. 1) and characteristic carboxylato vibration bands found in the range of $1430-1380\text{ cm}^{-1}$. A moderately intense band appeared at $\sim 3438\text{ cm}^{-1}$ and a relatively strong band at $\sim 1565\text{ cm}^{-1}$ could be ascribed to the N-H stretching and bending vibration mode of the $-\text{NH}_2$ group, respectively. IR spectrum of IRMOF-3-PA showed two new extra bands at $\sim 1651\text{ cm}^{-1}$ and $\sim 1617\text{ cm}^{-1}$; the former band could be ascribed to the characteristic vibration band for the azomethine group ($>\text{C}=\text{N}-$) whereas the latter one may due to the vibration mode of the $\text{C}=\text{N}$ bond of the pyridine ring. For IRMOF-3-PA-Cu, the vibration bands of both azomethine group and $\text{C}=\text{N}$ moiety of the pyridine ring were shifted to the lower frequency range and overlapped with the asymmetric band of the carboxylato group. This indicated coordination of azomethine nitrogen with copper metal ion. In addition, the catalyst showed two new bands at 485 and 417 cm^{-1} , which could be assigned to the asymmetric Cu-N stretching mode [32]. Two weak peaks at 364 and 306 cm^{-1} were obtained in the far IR range due to symmetric Cu-N stretching and Cu-Cl (terminal chloro) vibrations, respectively (Figure S8) [32].

To understand the authenticity and stability of all frameworks, powder XRD patterns of IRMOF-3, IRMOF-3-PA, and the catalyst were studied (Fig. 2). Their comparison with simulated IRMOF-3 confirmed

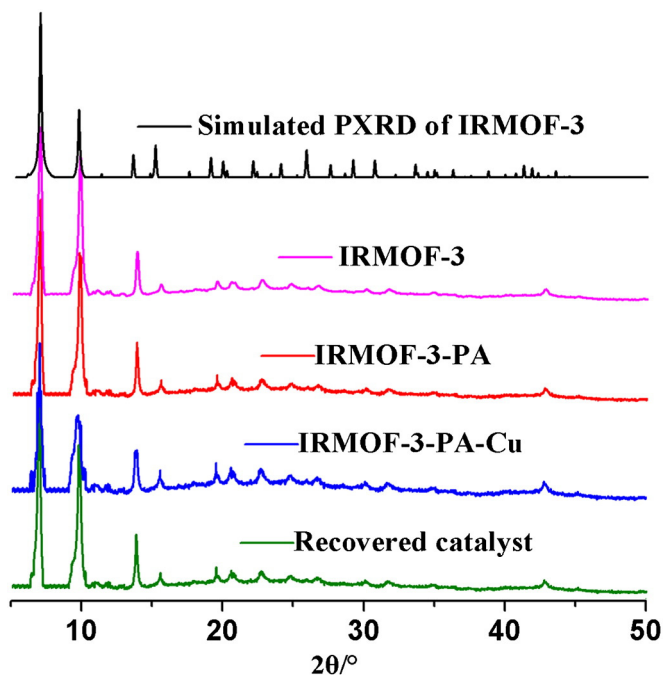


Fig. 2. PXRD pattern of 1 simulated, 1 synthesized, 2, 3 and 3 recovered.

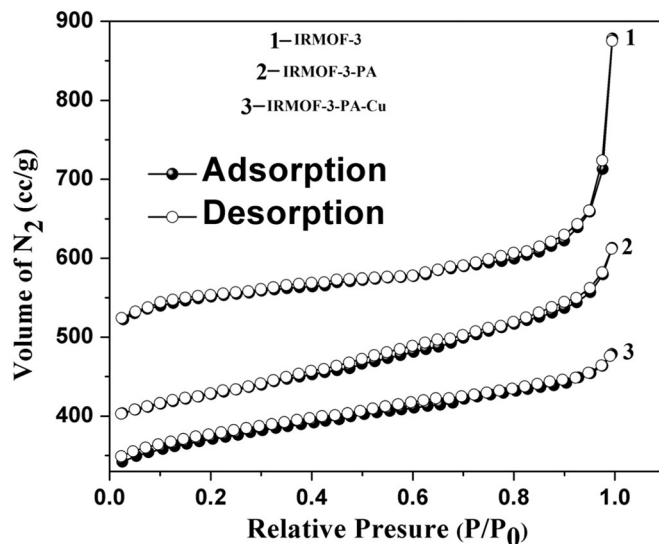


Fig. 3. Nitrogen sorption isotherms of (1) IRMOF-3, (2) IRMOF-3-PA and (3) IRMOF-3-PA-Cu at 77 K.

that organic functionalization as well as metalation had no effect on the structural integrity of the framework [30].

Comparison of EDX (Fig. 4C and D) analysis data of 2 and 3 indicates the presence of copper and chloride (ca. 1:2 ratio) along with zinc and oxygen in the catalyst. This ratio is close to coordination of copper with two chloride atoms as shown in Scheme 1.

Upon heating the catalyst showed a small weight loss between room temperature and $70\text{ }^\circ\text{C}$ (Figure S9) in thermogravimetric analysis. This can be due to the release of adsorbed solvent molecules. Thereafter TG curve remained flat indicating the thermal stability of the catalyst up to $\sim 230\text{ }^\circ\text{C}$.

The nitrogen sorption isotherms of IRMOF-3, IRMOF-3-PA and the catalyst were shown in Fig. 3; their pore diameter plot were given in Figure S10. BET surface area, pore volume and pore diameter data of all three species were collated in Table S1 and these values correspond well with literature data [33]. Gradual decrease of surface area, pore volume and diameter from IRMOF-3 to IRMOF-3-PA-Cu implied the inner surface modification of a solid framework.

The principle g values calculated from EPR spectrum of powdered IRMOF-3-PA-Cu (Figure S11) were in agreement with those reported for other copper(II) Schiff base complexes [34]. Copper(II) systems with $g_{\parallel} > g_{\perp} > 2.0023$ (2.42 and 2.06 respectively) suggested that the unpaired electron occupies the $d_{x^2-y^2}$ orbital, which was the characteristic of a square planar coordination environment of copper(II) [34].

3.2. Catalytic activity studies of 3

Initially, optimization studies for C-O cross-coupling reaction was undertaken using phenol and phenyl bromide as substrates under various reaction conditions as given in Table S2. Among different solvents, in DMSO the highest yield of product was obtained (entry 2). However, ethanol had been selected (entry 14) as solvent for its green nature. It had been found that O-arylation reaction was much faster with expensive Cs_2CO_3 than with K_2CO_3 or K_3PO_4 or Na_2CO_3 due to the enhanced basicity of Cs_2CO_3 (entries 8, 9, 11 and 14) and the catalyst was inactive in the absence of a base (entry 12) [35]. Considering temperature isolated yield was not up to the mark in low ($50\text{ }^\circ\text{C}$) temperature (entry 15). Thus the optimum condition of the catalytic reaction was as follows: Cs_2CO_3 (base), ethanol (solvent) and reaction temperature $80\text{ }^\circ\text{C}$.

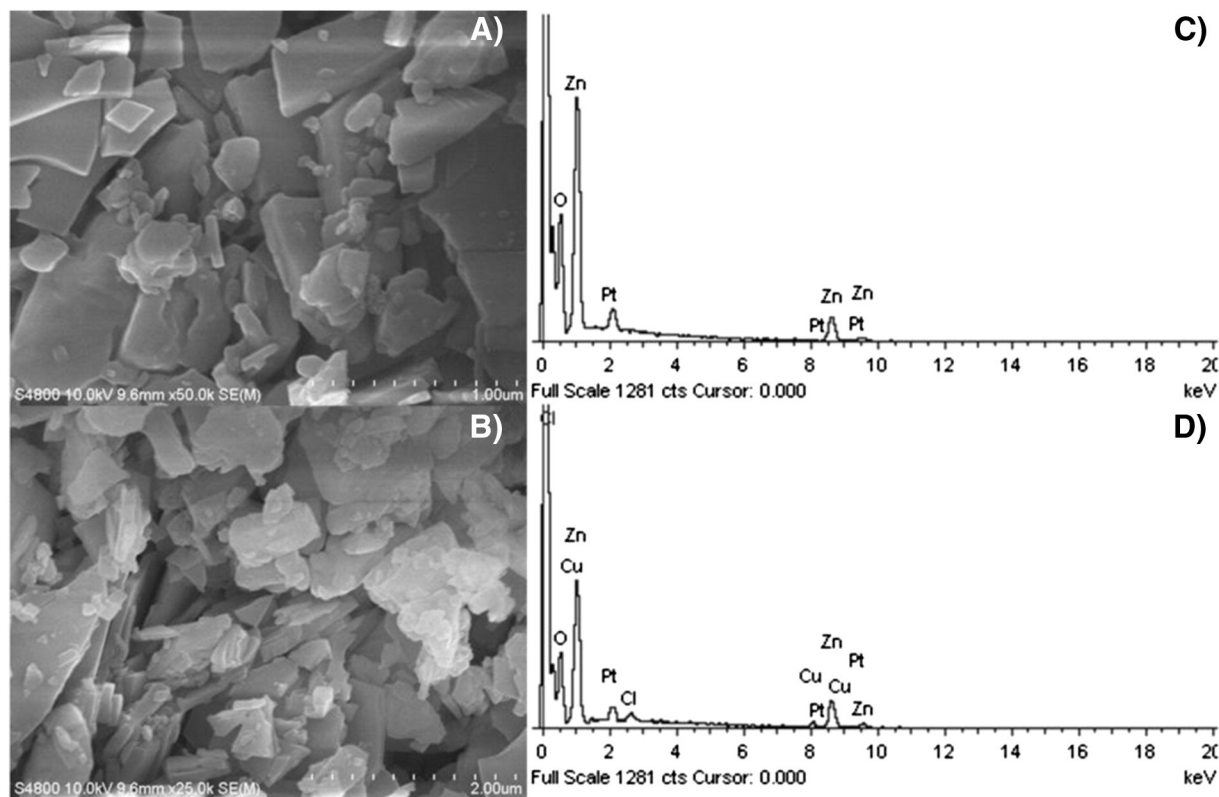


Fig. 4. SEM image and EDX spectra (A), (C) of 2 and (B), (D) of 3.

Notably, the reaction should be carried out under N_2 atmosphere as products yield decreases drastically in the air due to presence of moisture (entries 18 and 19). The catalyst showed that greater reactivity toward bromobenzene than iodobenzene may be due to the fact that I^- or I_2 generated from iodobenzene inhibits the catalytic process [26]. The catalyst was also capable of activating chlorobenzene (entry 21), however, yield was much lower than iodo- and bromobenzene. After completion of all reactions the conventional solvent extraction method was not employed to avoid hazardous organic solvents. Easy recycling of ethanol through controlled evaporation makes the reaction procedure more environment friendly.

Under optimized condition, we have employed various substrates to understand the efficacy of the catalyst in the C–O cross-coupling reaction (Table 1). Table 1 showed that substituent on the phenyl ring of both phenols and phenyl halides greatly influenced the reaction and displayed high to excellent yield of products. As ethanol (solvent) also contains oxygen atom, it can participate in C–O cross-coupling reaction to give a corresponding O-aryl product. But in our case we never faced such problem (entry 30). As illustrated in Table 1, α and β -naphthol reacted abnormally in our given reaction system (entries 25–29 and 20–24 for α and β -naphthol).

To ascertain if IRMOF-3-PA-Cu was responsible for such kind of anomalous positional-selectivity, we used ordered mesoporous silica immobilized heterogeneous catalyst SBA-15-TM-Cu (copper(II) anchored SBA-15) under the optimized condition (Table S3). We had undertaken a control experiment of O-arylation reaction using 1:1 mixture of α -naphthol and β -naphthol and equimolar *p*-bromonitrobenzene employing SBA-15-TM-Cu catalyst and compared results vis-à-vis those of IRMOF-3-PA-Cu. A cursory look at the results of catalytic reaction revealed that the yield of diaryl ethers of their corresponding reactants in SBA-15-TM-Cu catalyzed reactions were comparable, while, there was significant difference between those yields as catalyzed by IRMOF-3-PA-Cu. Being SBA-15-TM-Cu, a large-pore mesoporous silica, there were no space constraints for diaryl ether produced from both

α -naphthol and β -naphthol for diffusing out from the channel. However, this kind of diffusion for bulky substrates was not expected from the microporous IRMOF-3-PA-Cu. Therefore, it is reasonable to conclude that shape and size of the C–O coupling reaction products seems to be responsible for unexpected yield of desired products catalyzed by IRMOF-3-PA-Cu. To have a deeper insight into this we optimized the structure of the products by DFT calculations (Figure S12). Optimized dimensions of the diaryl ether molecules indeed support our point.

The catalyst IRMOF-3-PA-Cu was easily recoverable by centrifugation and could be reused several times without any significant loss of catalytic activity. As 0.002g of solid catalyst was not enough to recover, reuse, and finally characterize, the catalyst was collected from different batches of same catalytic cycle and an average value of data was reported here. The recycling test was performed with bromobenzene, phenol, CS_2CO_3 and maintained the optimized reaction conditions. After every cycle, the catalyst was recovered by centrifugation and then washed thoroughly with water–THF mixture solvent. The recovered catalyst was dried under vacuum at 130 °C overnight. Atomic absorption spectrometric analysis of the recovered catalysts confirmed the copper content of the IRMOF-3-PA-Cu remained the same. The catalyst IRMOF-3-PA-Cu could be reused up to five successive runs (shown in Fig. 5) without significant loss of catalytic activity. Different experiment and physico-chemical studies suggested that Cu was not being leached out from the solid catalyst during course of the reaction (see Supplementary content). The performance of IRMOF-3-PA-Cu had been compared with some previously reported heterogeneous Cu(II) systems, which catalyzed O-arylation reaction under a different catalytic condition (Table S4).

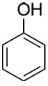
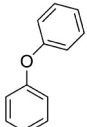
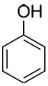
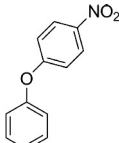
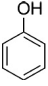
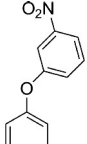
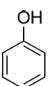
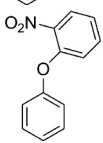
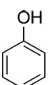
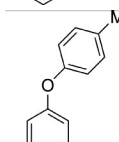
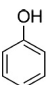
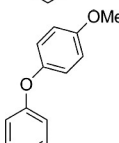
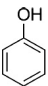
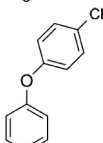
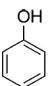
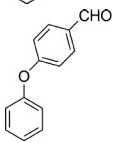
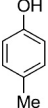
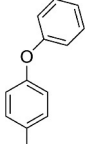
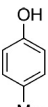
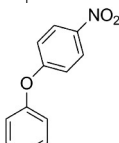
4. Conclusion

In essence, we have successfully synthesized a new heterogeneous catalyst by anchoring Cu(II) Schiff base moiety into porous IRMOF-3 by post-synthetic modification method. The reusable catalyst shows

Table 1

O-arylation reaction of different aryl alcohols with substituted aryl bromides^a

$$\text{Ar-OH} + \text{Br-C}_6\text{H}_3(\text{R}) \xrightarrow[\text{EtOH (2 ml), 80 }^\circ\text{C, 20 h, N}_2 \text{ atm.}]{\text{2 mg IRMOF-3-PA-Cu, Cs}_2\text{CO}_3 \text{ (1 mmol), 1.3 mmol}} \text{Ar-O-C}_6\text{H}_3(\text{R})$$

Entry	Aryl alcohol	R	Product	Yield ^b (wt.%)	TOF ^c (h ⁻¹)
1		H		77, 75 ^d	45, 43 ^d
2		p-NO ₂		90	53
3		m-NO ₂		85	50
4		o-NO ₂		88	51
5		p-Me		58	34
6		p-OMe		52	30
7		p-Cl		80	47
8		p-CHO		84	49
9		H		83	48
10		p-NO ₂		96	56

(continued on next page)

Table 1 (continued)

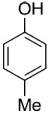
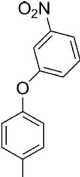
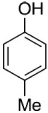
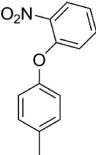
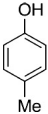
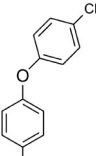
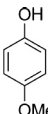
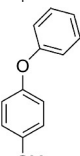
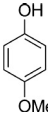
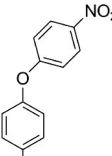
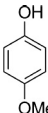
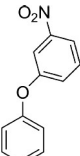
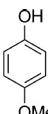
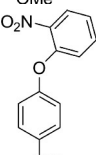
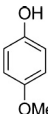
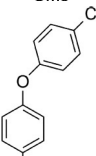
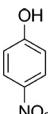
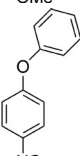
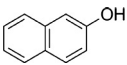
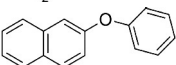
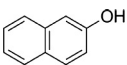
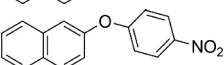
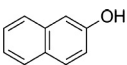
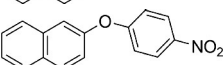
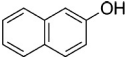
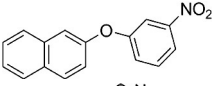
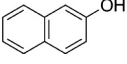
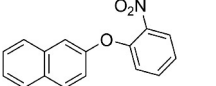
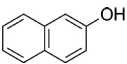
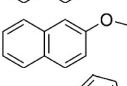
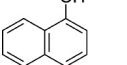
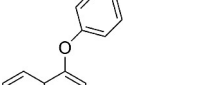
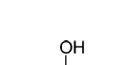
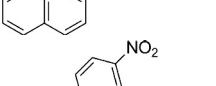
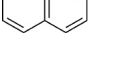
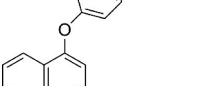
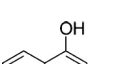
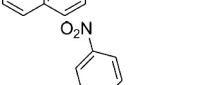
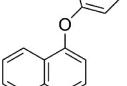
Entry	Aryl alcohol	R	Product	Yield ^b (wt.%)	TOF ^c (h ⁻¹)
11		m-NO ₂		92	54
12		o-NO ₂		95	55
13		p-Cl		90	53
14		H		86	50
15		p-NO ₂		98	57
16		m-NO ₂		94	55
17		o-NO ₂		95	55
18		p-Cl		92	54
19		H		63	37
20		H		67	39
21		p-NO ₂		87	51
22		m-NO ₂		77	45

Table 1 (continued)

Entry	Aryl alcohol	R	Product	Yield ^b (wt.%)	TOF ^c (h ⁻¹)
23		o-NO ₂		82	48
24		p-Cl		75	44
25		H		12	7
26		p-NO ₂		14	8
27		m-NO ₂		84	49
28		o-NO ₂		87	51
29		p-Cl		14	8
30 ^e	EtOH	H		-	-

^a Reaction condition: Aryl bromide (1.3 mmol), aryl alcohol (1.0 mmol), Cs₂CO₃ (1 mmol) and catalyst (0.002 g, Cu: 8.56×10^{-2} mol%) in EtOH (2 mL) at 80 °C for 20 h under N₂ atmosphere.

^b Isolated yield.

^c Mol. diaryl ether/mol. Cu h.

^d Fifth cycle.

^e Ethanol has been used in absence of aryl alcohol.

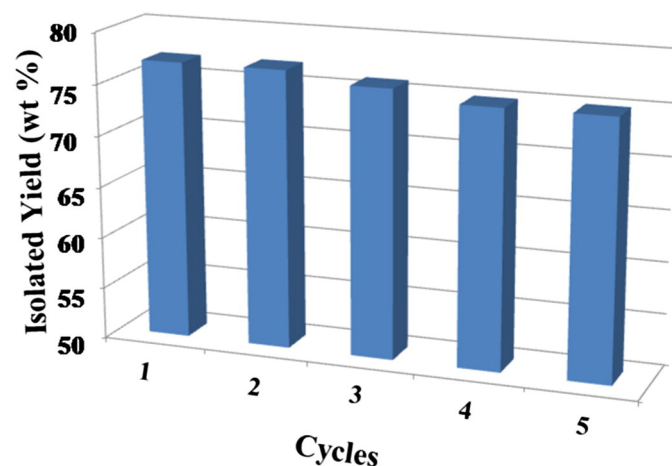


Fig. 5. Bar diagram showing recyclability of the catalyst.

high activity toward the O-arylation reactions of a variety of aryl alcohols with aryl bromides under relatively low temperature in green solvent. The functionalized pores of the catalyst are highly effective to cause a difference in the yield of products depending on their size.

Acknowledgments

Financial support from CSIR, New Delhi by a grant (Grant No. 01(2542)/11/EMR-II) (to S.K.) is gratefully acknowledged. T. M. thanks the Council of Scientific and Industrial Research (CSIR), New Delhi, for awarding him a fellowship.

Appendix A. Supplementary data

Supplementary data to this article can be found online at <http://dx.doi.org/10.1016/j.catcom.2014.09.006>.

References

- [1] N.T.S. Phan, T.T. Nguyen, C.V. Nguyen, T.T. Nguyen, *Appl. Catal. A Gen.* 457 (2013) 69–77.
- [2] S. Benyahya, F. Monnier, M.W.C. Man, C. Bied, F. Ouazzanib, M. Taillefer, *Green Chem.* 11 (2009) 1121–1123.
- [3] G. Mann, C. Incarvito, A.L. Rheingold, J.F. Hartwig, *J. Am. Chem. Soc.* 121 (1999) 3224–3225.
- [4] C.H. Burgos, T.E. Barder, H.X. Huang, S.L. Buchwald, *Angew. Chem. Int. Ed.* 45 (2006) 4321–4326.
- [5] L. Yin, J. Liedscher, *Chem. Rev.* 107 (2007) 133–173.
- [6] A. Naidu, G. Sekar, *Tetrahedron Lett.* 49 (2008) 3147–3151.
- [7] A.B. Naidu, E.A. Jaseer, G. Sekar, *J. Org. Chem.* 74 (2009) 3675–3679.
- [8] S. Lohmann, S.P. Andrews, B.J. Burke, M.D. Smith, J.P. Attfield, H. Tanaka, K. Kaneko, S.V. Ley, *Synlett* 8 (2005) 1291–1295.
- [9] S. Benyahya, F. Monnier, M. Taillefer, M.W.C. Man, C. Bied, F. Ouazzani, *Adv. Synth. Catal.* 350 (2008) 2205–2208.
- [10] T. Miao, L. Wang, *Tetrahedron Lett.* 48 (2007) 95–99.
- [11] J.T. Zhang, Z.H. Zhang, Y. Wang, X.Q. Zheng, Z. Wang, *Eur. J. Org. Chem.* (2008) 5112–5116.
- [12] M. Kidwai, N.K. Mishra, V. Bansal, A. Kumar, S. Mozumdar, *Tetrahedron Lett.* 48 (2007) 8883–8887.
- [13] S. Jammie, S. Sakthivel, L. Rout, T. Mukherjee, S. Mandal, R. Mitra, P. Saha, T. Punniyamurthy, *J. Org. Chem.* 74 (2009) 1971–1976.
- [14] J. Yang, P. Li, L. Wang, *Catal. Commun.* 27 (2012) 58–62.
- [15] J. Gascon, A. Corma, F. Kapteijn, F.X.L. i Xamena, *ACS Catal.* 4 (2014) 361–378.
- [16] R. Sen, D. Saha, S. Koner, *Chem. Eur. J.* 18 (2012) 5979–5986.
- [17] D. Saha, R. Sen, T. Maity, S. Koner, *Dalton Trans.* 41 (2012) 7399–7408.
- [18] D. Saha, T. Maity, R. Sen, S. Koner, *Polyhedron* 43 (2012) 63–70.
- [19] D. Saha, T. Maity, S. Das, S. Koner, *Dalton Trans.* 42 (2013) 13912–13922.
- [20] T. Maity, D. Saha, S. Das, S. Koner, *Eur. J. Inorg. Chem.* (2012) 4914–4920.
- [21] J. Lee, O.K. Farha, J. Roberts, K.A. Scheidt, S.T. Nguyen, J.T. Hupp, *Chem. Soc. Rev.* 38 (2009) 1450–1459.
- [22] A. Corma, H. Garcia, F.X.L. i Xamena, *Chem. Rev.* 110 (2010) 4606–4655.
- [23] O.M. Yaghi, M. Q'Keefe, N.W. Ockwig, H.K. Chae, M. Eddaoudi, J. Kim, *Nature* 423 (2003) 705–714.
- [24] M. Eddaoudi, J. Kim, N. Rosi, D. Vodak, J. Wachter, M. O'Keefe, O.M. Yaghi, *Science* 295 (2002) 469–472.
- [25] H. Li, M. Eddaoudi, M. O'Keefe, O.M. Yaghi, *Nature* 402 (1999) 276–279.
- [26] D. Saha, R. Sen, T. Maity, S. Koner, *Langmuir* 29 (2013) 3140–3151.
- [27] G.S. Yang, Z.L. Lang, H.Y. Zang, Y.Q. Lan, W.W. He, X.L. Zhao, L.K. Yan, X.L. Wang, Z.M. Su, *Chem. Commun.* 49 (2013) 1088–1090.
- [28] D. Zhao, J. Feng, Q. Huo, N. Melosh, G.H. Fredrickson, B.F. Chmelka, G.D. Stucky, *Science* 279 (1998) 548–552.
- [29] J. Huang, J. Yin, W. Chai, C. Liang, J. Shen, F. Zhang, *New J. Chem.* 36 (2012) 1378–1384.
- [30] J.G. Nguyen, S.M. Cohen, *J. Am. Chem. Soc.* 132 (2010) 4560–4561.
- [31] S.M. Cohen, *Chem. Rev.* 112 (2012) 970–1000.
- [32] P.F. Rapheal, E. Manoj, M.R.P. Kurup, *Polyhedron* 26 (2007) 818–828.
- [33] M. Zhao, K. Deng, L. He, Y. Liu, G. Li, H. Zhao, Z. Tang, *J. Am. Chem. Soc.* 136 (2014) 1738–1741.
- [34] S. Koner, *Chem. Commun.* (1998) 593–594.
- [35] B. Schlummer, U. Scholz, *Adv. Synth. Catal.* 346 (2004) 1599–1626.